Evaluating decadal space-temporal mangrove dynamics using geographic object-based image analysis (GEOBIA) on the Doce River delta-ES, southeastern Brazilian coast

Débora Cristina De Lima Miranda, Marlon Carlos França, Luke Ortiz-Whittingham, Laurent Polidori

Quaternary Science Advances 13 (2024) 100149

Contents lists available at ScienceDirect

Quaternary Science Advances

journal homepage: www.sciencedirect.com/journal/quaternary-science-advances

Evaluating decadal space-temporal mangrove dynamics using geographic object-based image analysis (GEOBIA) on the Doce River delta-ES, southeastern Brazilian coast

Débora Cristina de Lima Miranda [a,*], Marlon Carlos França [a,b,c], Luke Ortiz-Whittingham [d], Laurent Polidori [a,e]

[a] Graduate Program of Geology and Geochemistry, Federal University of Pará, Av. Perimentral 2651, Terra Firme, CEP: 66077-530, Belém, PA, Brazil
[b] Laboratory of Oceanography and Climate, Federal Institute of Espírito Santo, Rua Augusto Costa de Oliveira, 660, Piúma, ES, Brazil
[c] Department of Earth, Geographic and Climate Sciences, in the School of Earth and Sustainability Geosciences at the University of Massachusetts, Amherst, MA, 01003, United States
[d] Amherst College, Amherst, MA, 01003, United States
[e] CESBIO, Université de Toulouse, CNES/CNRS/INRAE/IRD/UPS, Toulouse, France

ARTICLE INFO

Keywords:
Mapping
Geobia
Remote sensing
Mariricu river
Accuracy
Mangrove

ABSTRACT

Mangroves are ecosystems present in a large part of the Brazilian coastal zone that are home to a wide diversity of organisms, providing direct and indirect resources, as well as nursery and foraging habitats. Using images in 5-year intervals (2010, 2015, and 2020), the present study carried out a decadal mapping of the remaining mangroves of the Doce River delta along the tidal flats of the Mariricu River, in the coastal region of the city of São Mateus-ES. In this context, object-oriented classification methodology (GEOBIA) was used, which allowed the generation of high-resolution data. This methodology achieved excellent results, as evidenced by the global accuracy numbers and Kappa index, which gave an average of 96.78% and 93.5% respectively; and by low values of disagreement, with an average of 3.22%. The change detection analysis showed alterations in the landscape over time, with 9% of the mangrove areas becoming extinct, 12% of the areas expanding, and 79% of the areas remaining preserved. Therefore, our mapping data are consistent with the data published by the State Institute for the Environment and Water Resources of the State of Espírito Santo (IEMA), as well as with scientific works that recorded areas of reduction and expansion for mangroves, but mostly with large preserved areas. With that, our results demonstrate the highly effective application of geotechnologies for coastal environmental analyses with low cost and high speed.

1. Introduction

Mangroves are found in tropical and subtropical regions of coastal zones, between latitudes 30° N and 30° S (Giri et al., 2011), distributed in protected regions and along estuary margins (Tomlinson, 1986; Duke et al., 1998). Brazil has the second largest mangrove area in the world (Bezerra et al., 2022), occupying approximately 10,020 km^2 (Diniz et al., 2019) between 4°20′N, Oiapoque-AP, and 28°30′S, Laguna-SC (ICMBio, 2018).

Mangrove ecosystems are among the most productive and biologically important in the world (Woodroffe et al., 2014). In addition to acting significantly in carbon sequestration (Alongi, 2012; Howard et al., 2017). Especially Brazil's mangrove soil currently stores about 3–8% of global carbon (Hatje et al., 2021). They also provide essential goods and services for society and for the maintenance of marine coastal systems, including stabilization of coastlines, as well as protection against tsunamis and hurricanes (Kathiresan and Rajendran, 2005; Alongi, 2008, 2012; Kristensen et al., 2008; Giri et al., 2011). Physical-chemical factors are determinant for the development and permanence of mangroves, which, in general, develop better where the adequate topography is subject to a large tidal range and large inflows of water from rivers, rain, nutrients and sediments (Schaeffer-Novelli et al., 1990). These ecosystems are particularly sensitive to climate and environmental changes (Alongi, 2015), and are used as indicators to investigate coastal changes (Blasco et al., 1996).

The global distributions of mangroves have undergone variations

* Corresponding author.
E-mail address: deborramiranda@gmail.com (D.C. Lima Miranda).

https://doi.org/10.1016/j.qsa.2023.100149
Received 30 June 2023; Received in revised form 18 November 2023; Accepted 27 November 2023
Available online 1 December 2023

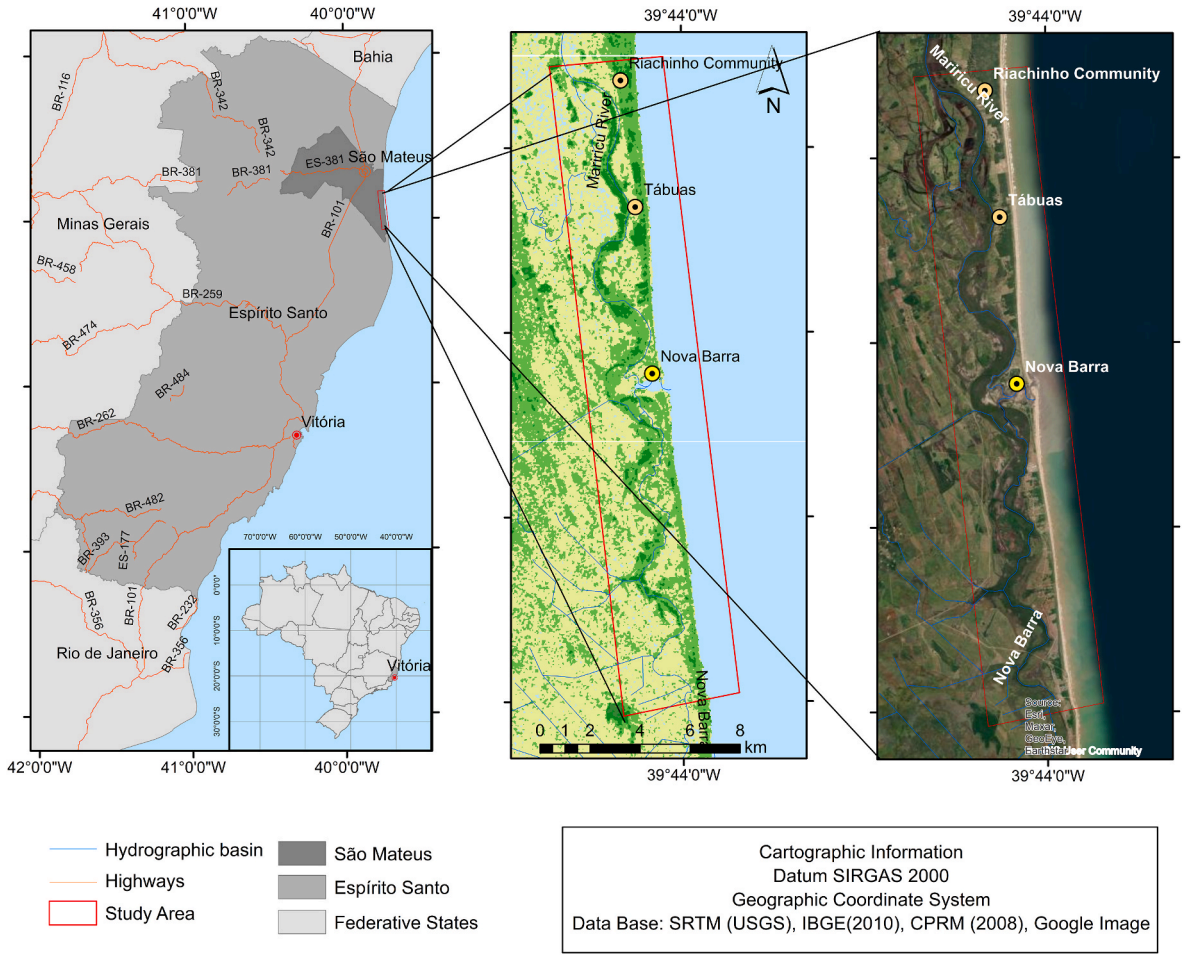

Fig. 1. Study area.

during geological and human history, as a result of global climate change, variations in relative sea level (RSL), and sediment dynamics (Fromard et al., 2004; Cohen et al., 2012). According to Suguio et al. (1985), a set of sedimentological and biological evidence can reveal these variations.

Paleoenvironmental studies have been developed along the Brazilian coast (Cohen et al., 2012; França et al., 2012; Rodrigues et al., 2022; Nunes et al., 2023), including the Doce River delta (França et al., 2016; Silva et al., 2022, 2023), located in the state of Espírito Santo, southeastern Brazil. These studies allow a better understanding of climate change and variations of RSL reflected in mangrove systems (Castro et al., 2013; Cohen et al., 2014; Rossetti et al., 2015; França et al., 2016).

The Doce River delta has undergone several geological events, and within sediments can be found traces of this history. For example, Rossetti et al. (2015) describe three progradation events in the deposition of beach ridges phases and two transgressive events in the deposition of transgressive sediments, the latter set of events being registered in the sediments present in the mangrove forests.

Mapping mangrove areas, obtaining quantitative data from these areas, and identifying the intensity of changes is extremely important, as these ecosystems are areas that guarantee the reproduction of aquatic species; the quality of life of local, regional and global communities; food availability, improvement of air quality, and stabilization of the coastline, in addition to the maintenance and promotion of tourist activities (Friess et al., 2019; Van der Stocken et al., 2019; Hamylton et al., 2023).

The geotechnologies available today are essential instruments for monitoring transformations in geographic space (Felgueiras, 2001). Environmental modeling, developed with remote sensing data and geoprocessing techniques, allows us to study the past and the present, in the quest to better understand the dynamics, what they entail, and what we can do to maintain or accelerate them, according to human and/or natural needs.

The GEOBIA method (object-oriented classification) combines the contextual analysis of visual interpretation with the quantitative aspect of pixel-based approaches, like a classical method for remoting sensing analysis (Kamal et al., 2015; Hidayatullah et al., 2023; Kundal et al., 2023). It is defined by analyzing the image and segmenting it into objects by grouping similar contiguous pixels, delimiting boundaries with homogeneous regions (Desclée et al., 2006).

In analyzing the image, the GEOBIA takes into account the user's knowledge, integrating several data sources and making available object-images from physical and abstract information. This information includes natural and anthropogenic forms, such as those from the cultures that may have originated them (Hay and Castilla, 2008; Blaschke et al., 2014).

Studies like Nascimento et al. (2013), Carvalho de et al., (2015), Eugenio et al. (2017), Freitas et al. (2017), Diniz et al. (2019), and Lopes (2020) mapped the macro-, meso- and micro-tide mangroves along the Brazilian coast, revealing the variations of the areas in different time intervals.

Despite the Doce River delta being extensively studied, carrying out a mapping study of areas that have not yet been cataloged is of essential importance for a broader understanding of which areas are being most and least impacted in terms of mangrove forest variations. Such a study would serve as a scientific basis for understanding the dynamics of areas of growth and decline/extinction of these ecosystems, thus offering an interpretation of the data for detecting changes in the mangrove area

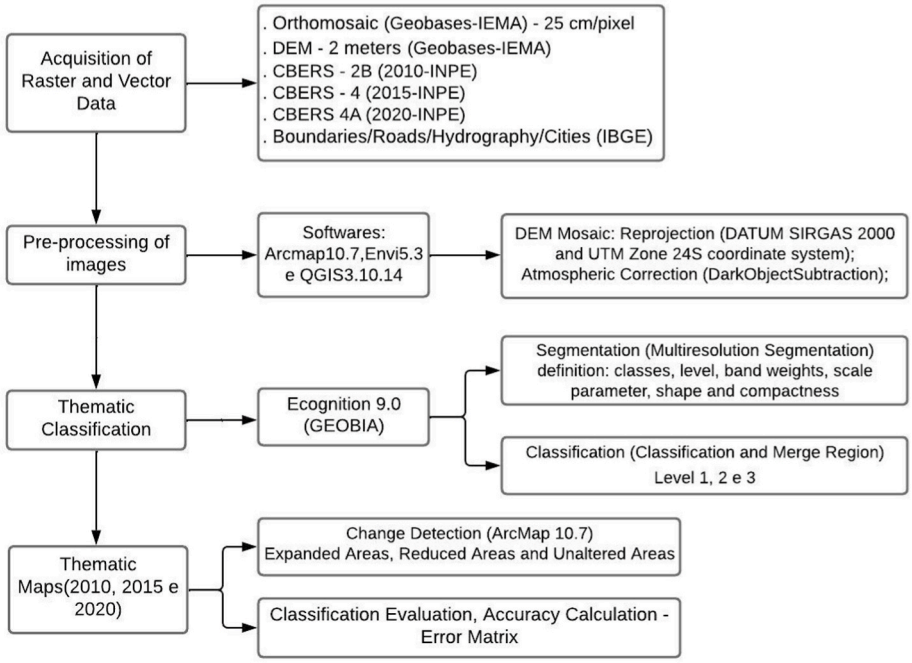

Fig. 2. Flowchart for the methods.

over the course of the decade.

Therefore, considering the hypothesis of recent mangrove dynamics on the southeastern Brazilian coastal region, the goal of this work is to evaluate the classification and identify areas of expansion and contraction of mangroves on the Doce River delta over the course of a decade (2010, 2015 and 2020), based on geographic object-based image analysis (GEOBIA), digital elevation model (DEM), and optical images, in order to provide a pioneering work of great importance for the consolidation of an overview of the area, which can be used as a tool for coastal management.

2. Study area

2.1. Location

The study area is located between the geographic coordinates 39°45′21″W 19°4′18″S and 39°46′59″W 18°50′14″S that delimit the polygon with approximately 119.5 km^2–80% on dry land and 30% on oceanic and/or estuarine waters located in northeastern Espírito Santo State (Fig. 1). The study area is located in a warm and humid tropical climate, with annual precipitation 1190 mm, approximately, and temperature ranges between 20° and 25 °C (Buso-Junior et al., 2013). Precipitation occurs mainly during the summer (November–January), while the winter is characterized by a dry season (May–September), according to Carvalho et al. (2004). Most of the study area is occupied by mangrove trees, ~5–10 m tall, represented by *Rhizophora mangle*, *Laguncularia racemosa*, and *Avicennia germinans*. The sandy coastal plain flora is characterized by restinga ecosystems and herbaceous vegetation (França et al., 2016; Silva et al., 2022).

Table 1
Tables with all the acquired data that were used in the mapping, highlighting their characteristics.

SATELLITE/SENSOR	TYPE	PLATFORM	WAVELENGTH OF BANDS	PIXEL SIZE	DATE	CAMERA	RANGE IMAGING
CBERS 2B	optical	Satellite	0,51 - 0,73 μm (pan) 0,45 - 0,52 μm (blue) 0,52 - 0,59 μm (green) 0,63 - 0,69 μm (red) 0,77 - 0,89 μm (near infrared)	20m	02/16/2010	CCD	113 km
CBERS 4	optical	Satellite	0,45-0,52 μm (B) 0,52-0,59 μm (G) 0,63-0,69 μm (R) 0,77-0,89 μm (NIR)	20m	10/13/2015	MUX	120 km
CBERS 4	optical	Satellite	0,51-0,85 μm (Pan) 0,52-0,59 μm (G) 0,63-0,69 μm (R) 0,77-0,89 μm (NIR)	5m	09/17/2015	PAN	60 km
CBERS 4A	optical	Satellite	0,45-0,52 μm (B) 0,52-0,59 μm (G) 0,63-0,69 μm (R) 0,77-0,89 μm (NIR) 0,45-0,90 μm (PAN)	2 m (PAN) 8 m (others)	July 08, 2020	WPM	92 km
DEM	Optical	Aircraft		2m	2012–2015		
Orthomosaic	Optical	Aircraft		25 cm	2012–2015		

3. Materials and methods

3.1. Data acquisition

The classification of satellite images was performed according to the object-oriented classification methodology (GEOBIA), with an interval of 5 years for each year worked and a temporal space of one decade. The steps followed to reach the final result are schematized in Fig. 2.

The images used were acquired on the free platform of the INPE image catalog that provides images from the CBERS satellite. The images are organized thus: CBERS 2B images are from 2010, CBERS 4 from 2015, and CBERS 4A from 2020. After processing, the images have a resolution of 20, 5, and 2 m, respectively, with properties and characteristics described in Table 1.

Other data used in the work were: (1) an orthomosaic with a resolution of 25 cm/pixel in RGB (true color) articulated in blocks of 10 × 10 km, elaborated through the differential rectification of aerial photographs based on a digital elevation model (DEM); and (2) a digital elevation model (DEM), i.e., a three-dimensional representation of the Earth's physical surface with a 2 m pixel size, automatically generated by digital photogrammetry (IEMA, 2015). Both were prepared between 2012 and 2015 under the Mapping ES 2012–2015 project, by the company Hiparc Geotecnologia contracted by the Institute of Environment and Water Resources (IEMA, ES, Brazil), acquired on the platform of the Integrated System of Geospatial Bases of the State of Espírito Santo (GEOBASE).

Vector data were also used, such as shapes of town, state and federal boundaries, as well as roads, hydrography and cities obtained from the IBGE and IEMA databases.

Table 2
Dispositions of the classes and characteristics.

CLASS	IMAGE (COLORED COMPOSITION R3NIR4B1)	TEXTURE, COLOR, SHAPE, SIZE	LOCATION/ CONTEXT
Fluvial/ Estuarine water	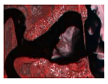	Smooth texture, dark color, with elongated meandering shapes and sizes considered large.	It occupies the central part of the image, always connected to the mangrove class and connected to the ocean by an estuarine channel.
Restinga		Rough texture, bright red color, with rectilinear shapes, of varying sizes.	Most of them appear next to the beach class, and irregular in shape throughout the image.
Mangrove	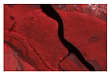	Smooth texture, darker red color, meandering shapes with large rounded edges.	Inserted in the center of the image, always linked to the fluvial water class.
Beach		Smooth texture, whitish coloring, large rectilinear shapes.	To the right of the image, linked to the class vegetation and oceanic waters.
Sea		Rough texture, navy blue color, irregular shape and large size.	The extreme right of the image, and occurs always connected with the beach class.
Farms		Irregular texture, grayish red color varying to light red with white dots, irregular shape and size.	Arranged over the entire image area, linked to various classes.

3.2. Pre-processing

The acquired images went through pre-processing processes to be used later in the classification, going through the following treatments.

- Mosaic: The DEM images were mosaicized with a total of six scenes that covered the entire study area, where they were later cut out on the perimeter of the polygon of interest; this was carried out in the Arcmap 10.7 software using the Mosaic to New Raster tool;
- Reprojection: All data acquired except the orthomosaic and the DEM present original projection DATUM WGS1984 and UTM Zone 24S coordinate system. It was necessary to reproject the data for the current Brazilian system with DATUM SIRGAS2000 and UTM Zone 24S coordinate system. This reprojection was performed on the QGIS 3.10.14 software platform;
- Atmospheric correction: In the CBERS 2B, CBERS 4 and CBERS 4A images, atmospheric correction was performed using the Dark Object Subtraction method from the Envi5.3 software, which aimed to improve the quality of the images by eliminating radiometric distortions caused by the atmosphere.

The main evidence of atmospheric effects on the image are the decrease in surface brightness in specific spectral regions and the presence of haze, with loss of sharpness in regions of shorter wavelengths. When passing through the atmosphere, radiation from the sun interacts with it, causing changes in its propagation, called scattering and absorption (Latorre et al., 2002).

According to (Meneses and Almeidaorg, 2012) the atmosphere affects the radiance measured at any point in the image in two apparently contradictory ways: first, it acts as a reflector, adding an extra radiance to the signal that is detected by the sensor; second, it acts as a spotter, attenuating the intensity of energy illuminating the surface target. Another important factor is the so-called additive effect (haze) of the scattering of rays caused by aerosols, gases and water molecules in the atmosphere, which reduces the contrast of the image.

The Dark Object Subtraction (DOS) method chosen to be applied to the CBERS images brought good results. According to Moses et al. (2017), the technique assumes that the images contain at least a few dark pixels, where the radiance on the sensor can be completely attributed to the atmospheric contribution and specular reflection from the water surface, so the DOS method looks for the lowest radiance in each spectral band over the entire image which is taken as the dark pixel radiance. The dark pixel radiance is then subtracted from the radiance on the sensor for all pixels.

The ideal method to perform the atmospheric correction would be one that uses in situ or real information, however most users employ previously collected remote sensing data, and although the DOS technique is considered simple it only requires information contained in the digital image data, where it involves the subtraction of a constant DN value (digital number) in the image (Chavez, 1988).

The fusion method was used in the images developed to improve the spatial resolution, using the pansharpening tool available on the Arcmap 10.7 software platform. It was possible to achieve an improvement in resolution from 20 m to 5 m in the CBERS 4 image and from 8 m to 2 m in the CBERS 4A image. The technique makes it possible to integrate the best spatial resolution of the panchromatic band with the best spectral resolution of the other bands, producing color images that combine both characteristics (Leonardi and Oliveira, 2009).

3.3. Thematic classification

To obtain the classified images of the proposed years, we employed the object-oriented classification (GEOBIA). GEOBIA is described by Hay and Castilla (2008) as a subdiscipline of Geographic Information Science (GIScience) dedicated to the development of automated methods to partition remote sensing images into significant object-images and

Table 3
Classification processing tree.

LEVEL	PROCESS	SON PROCESS	ALGORITHM	FUNCTION	THRESHOLDS		
					2010	2015	2020
1	Segmentation	Image Segmentation	*Multiresolution Segmentation*	___	___	___	___
	Classification	Classify not Continent	*Classification*	10* ln ([Mean DEM])	≥ - 58 ≤ - 20	≥ - 58 ≤ - 20	≥ - 58 ≤ - 20
		Classify Continent		10* ln ([Mean DEM])	≥ - 3	≥ - 3	≥ - 3
2	Copy Classification	Copy Level 1 Classification	*copy image object level*	___	___	___	___
	Classification	Classify Vegetation	*Classification*	(([Mean B4-NIR]-[Mean B3])/([Mean B4-NIR]+[Mean B3]))*100 (NDVI)	≥ - 32	≥ - 32	≥ - 32
		Classify No Vegetation		(([Mean B4-NIR]-[Mean B3])/([Mean B4-NIR]+[Mean B3]))*100 (NDVI)	≤ - 32	≤ - 32	≤ - 32
3	Copy Classification	Copy Level 2 Classification	*copy image object level*	___	___	___	___
	Classification	Classify Restinga	*Classification*	10*ln(Mean DEM)	≥ 20.2 ≤ 30	≥ 20.2 ≤ 30	≥ 20.2 ≤ 30
		Classify Farms		10*ln(Mean DEM)	≥ 4 ≤ 18	≥ 4 ≤ 18	≥ 4 ≤ 18
		Classify Mangrove		[(10* lg ([Mean B4-NIR])+(10* ln ([Mean DEM])] (Nascimento et al., 2013)	≥ 26.5 ≥ 20	≥ 26.5 ≥ 20	≥ 26.5 ≥ 20
		Classify Sea		10* ln ([Mean DEM])	≥ - 58 ≤ - 20	≥ - 58 ≤ - 20	≥ - 58 ≤ - 20
		Classify Fluvial Water	*Assign Class By Thematic Layer*	___	___	___	___
		Classify Beach		___	___	___	___
	Reclassification	Distinguish Mangrove from Restinga	*Classification*	Rel. bord to Fluvial Water	≥ 0.4	≥ 0.4	≥ 0.4
	Agroup classes	___	*Merge Region*	___	___	___	___

evaluate their characteristics through spatial, spectral and temporal scales, in order to generate new geographic information in a GIS-ready format.

The GEOBIA classification does not build tools, but it generates geographic information, which allows users to interpret and respond effectively to some specific problem, such as global climate change, natural resource management, land use/land cover mapping, among others (Hay and Castilla, 2008).

For Hay and Castilla (2008), Antunes (2015), and Trimble, (2014), the GEOBIA method presents many benefits and advantages, such as the ability to iteratively create an image, recognizing groups of pixels as objects. It also provides an analogy to the human mind, using the color, shape, texture, and size of objects, in addition to the context and relationships of the landscape.

The software used was Definions e-Cognition, which extracts the meaning of connotations and mutual relationships of objects, not only from neighbors but from various input data. The software has algorithms for analyzing the following different aspects: multiresolution segmentation, where weight is assigned to the bands according to the spectral response ranging from 0 to 1; segmentation scale and shape; and compactness. Other aspects analyzed by the algorithm were the classification, stage of defining, and hierarchical ordering of classes, which were modeled by fuzzy relevance rules, in addition to merging regions, the final process of grouping objects belonging to the same classes.

3.3.1. Segmentation

At this stage, the CBERS images were analyzed and carefully observed to define all the classes to be mapped, taking into account properties such as: texture, color, shape, size, location and context. In addition to the visual analysis, the mapping and orthomosaic of the region, prepared by IEMA in 2012 at a scale of 1:25,000 (the same used in this work), was evaluated and considered, which allowed a good

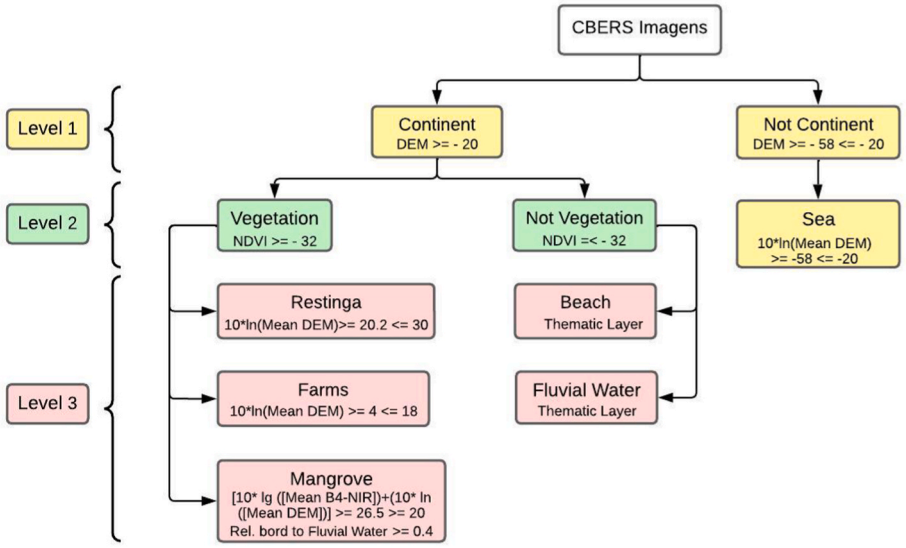

Fig. 3. Applied hierarchy in classification.

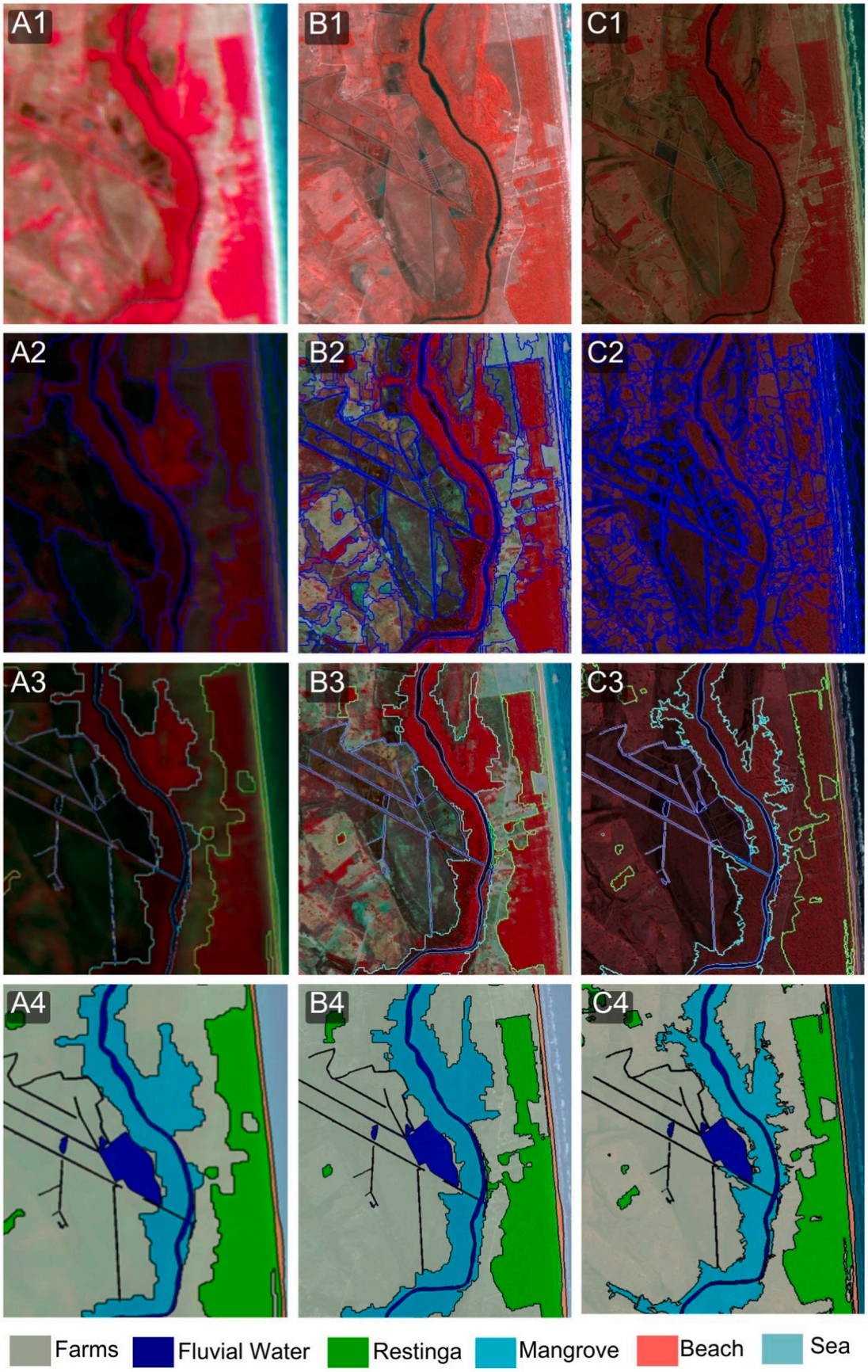

Fig. 4. Classification process. A1, B1, C1 - reference images of the three R3NIR4B1 periods. A2, B2, C2 - segmentation of images into objects, with different sizes of objects being visualized in response to the difference in resolution of the images. A3, B3, C3 - merge of objects of the same class, A4, B4, C4 - final classification.

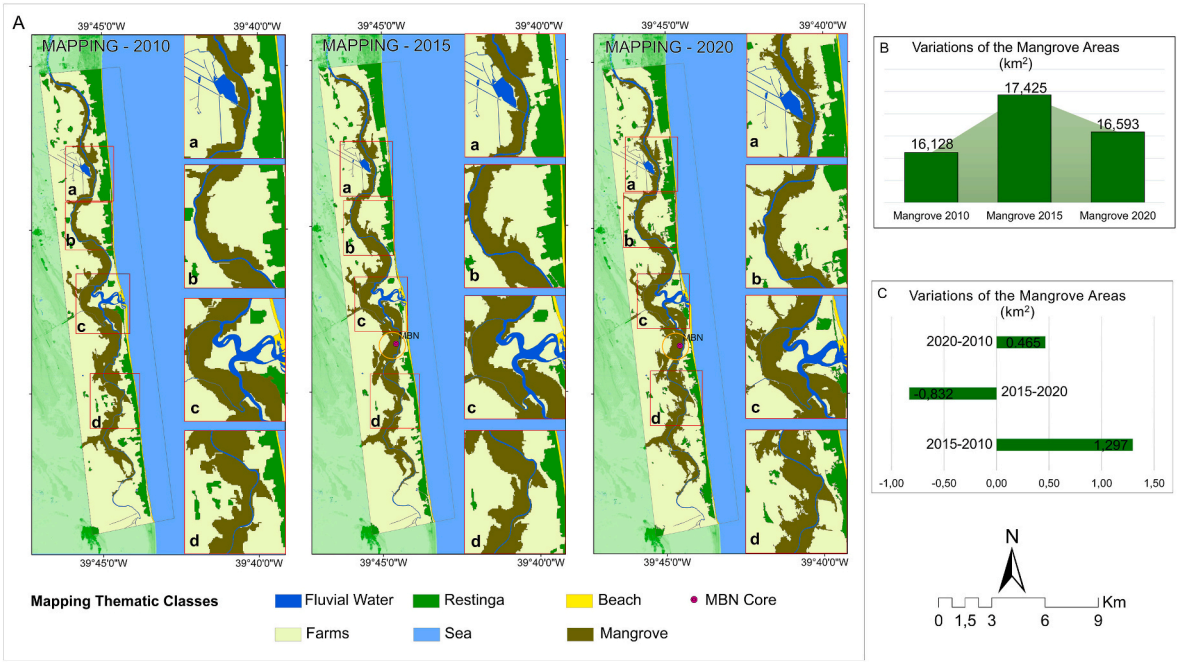

Fig. 5. a - Classification of the years 2010, 2015 and 2020. B- Graphic of changes in mangrove areas in m^2, in the years 2010, 2015 and 2020. C- Gain and loss of mangrove areas in m^2, in the years of 2010, 2015 and 2020.

support for the definition of classes. Table II describes all defined classes as well as their characteristics that helped in the differentiation.

Adapting the method proposed by Nascimento et al. (2013), the segmentation process took place at level 1, and after several tests a combination was found that most highlighted the defined classes. The CBERS images received weight 1 for the blue (B1), green (B2) and red (B3) bands and weight 5 for the near infrared (NIR) band, since the latter better reflects forest areas. Parameter scale 135, for shape 0.1, and compactness 0.5.

3.3.2. Classification

In the classification stage, several factors were taken into account, such as defined levels, class hierarchy, types of processes, algorithms, functions and thresholds, which define the processing tree shown in Table III.

The classification was carried out according to hierarchy levels schematized in Fig. 3. In the classification level 1, the continent and non-continent areas were defined, using the DEM as a tool, with the purpose of better defining the coastline. At level 2, the continental regions were distinguished between areas of vegetation and non-vegetation, using the normalized difference vegetation index (NDVI) as the main criterion, which evaluates the condition of the vegetation through multispectral images.

At level 3 all other classes were classified, separating the vegetation into native vegetation, farm area and mangrove vegetation. To distinguish the first two, the DEM was used, as the classes differed greatly in the topographic elevations, with the native vegetation class (restinga) between the highest levels and the undergrowth (use area) with the lowest. The mangrove vegetation was distinguished from the others through band mathematics with a function developed by Nascimento et al. (2013), using the NIR band and the DEM, together with the criteria of proximity to the hydrography, where the mangrove vegetation stood out for occupying the areas closest to the fluvial drainage.

Areas previously classified as non-continental were reclassified as sea using the same tools and thresholds. The beach and fluvial water classes were classified using shapefiles through the Thematic Layer tool provided by IEMA. Fig. 4 shows the processes described above, going from the original treated image to segmentation into objects, merging of segmented objects and final classification.

3.4. Detection of changes

The change detection process was carried out through an adaptation of the methodology employed by Weckmüller and Vicens (2013), using the "from-to" technique. Using the GIS environment of the ArcMap 10.7 software, the maps produced in eCognition in vector format were inserted; and analyses and data crossing were processed using the intersect tool, locating exactly the regions that underwent changes.

To highlight the mangrove class, the main object of this study, all other classes such as area of use, restinga, beach, fluvial water and sea were grouped and reclassified as "other class," so only the mangrove class was analyzed, putting in evidence the regions that have suffered losses and increases in mangrove forests, as well as areas that have managed to remain unchanged over the years.

3.5. Evaluation of classifications

There is a strong consolidated bibliography regarding the evaluation of remote sensing image classifications, where the error matrix is the main instrument of this analysis. The error matrix works with the produced and reference data, providing a value of the global accuracy of the classification and the accuracy of the producer and the user, reaching the commission and omission error (Story and Congalton, 1986). Kappa statistics is also used as a tool for classification analysis (Congalton, 1991), in addition to the calculation of the Kappa index for each mapped class (Congalton and Green, 2019). Despite the wide acceptance of Kappa statistics in the specialized bibliography, Pontius and Millones (2011) describe that in a classification there may have been allocation disagreements, when there is a positional change of the pairs of pixels arranged in the classified map. Despite the amount disagreement, when the error occurs in the number of classified pixels.

In this way, the confusion matrices of the three years studied (2010, 2015, and 2020) were generated, bringing information on the number of reference points, producer and user accuracy, omission and commission errors, Kappa and Kappa indexes by class and the global accuracy, besides the values of the allocation and quantity disagreements.

Table 4
Confusion Matrix: Producer and User Accuracy Data, Global Accuracy and Kappa Index – a) year 2020, b) 2015 and c) 2010.

Classification	Mangrove	Others	Total	User Accuracy	Comission Error (%)
Mangrove	143	3	146	97.95	2.05
Others	7	147	154	95.45	4.55
Reference points	150	150	300		
Producer Accuracy (%)	95.33	98.00			
Omission error (%)	4.67	2.00			
KI for class	0.96	0,91			
Global accuracy	96.67%		Kappa Index	93.33%	

b)

Classification	Mangrove	Others	Total	User Accuracy	Comission Error (%)
Mangrove	143	2	145	98.62	1.38
Others	7	148	155	95.48	4.52
Reference points	150	150	300		
Producer Accuracy (%)	95.33	98.67			
Omission error (%)	4.67	1.33			
KI for class	0.97	0.91			
Global accuracy	97.00%		Kappa Index	94.00%	

c)

Classification	Mangrove	Others	Total	User Accuracy	Comission Error (%)
Mangrove	143	3	146	97.95	2.05
Others	7	147	154	95.45	4.55
Reference points	150	150	300		
Producer Accuracy (%)	95.33	98.00			
Omission error (%)	4.67	2.00			
KI for class	0.96	0.91			
Global accuracy	96.67%		Kappa Index	93.33%	

3.6. Data acquisition for accuracy calculation

To perform the accuracy analysis through the error matrices, it was necessary to analyze the classification regarding the error and hit statistics through the confusion matrix proposed by Story and Congalton (1986). For this, in ArcMap 10.7 software, random points were generated and sufficiently representative across the entire work area. Thus, a total of 300 points were randomly obtained for each classification for the years 2010, 2015 and 2020, divided between the mangrove and others classes (the latter class formed by grouping together the area of use, restinga, beach, ocean water, and fluvial water classes), in which 150 reference points correspond to the mangrove class and 150 points to the others class.

4. Results

4.1. Classification

According to the proposed methodology, based on object-oriented classification (GEOBIA), the final classifications of the proposed years were reached, with the mapping of six main classes, namely: Mangrove, Farms, Restinga, Beach, Fluvial Water and Sea (Fig. 5a).

The class of greatest interest in this work is located in the central portion of the mapped area. It differs from other vegetation because, in addition to presenting a higher NDVI value, it has a more imposing canopy than the area that stands out in the DEM. It differs also by its characteristic spatiality, where it is possible to identify that the class borders and follows a proximity to the river water class; thus, all factors were decisive for differentiating the class from other vegetation.

Statistically, we can observe that the mangrove vegetation has undergone variations over the years. In the years 2010, 2015 and 2020, areas of 16.128 km^2, 17.425 km^2 and 16.593 km^2 were mapped (Fig. 5b), respectively. Between 2010 and 2015, we observed that the mangrove forest grew by around 1297 km^2. However, in the period from 2015 to 2020, we observed a loss of 0.832 km^2 of mangrove forests. When analyzing the two extremes between the years 2010–2020, we identified a growth of 0.464 km^2 of mangrove forests (Fig. 5c).

4.2. Classification accuracy

Following the described methodology, among the 300 reference points collected in the images of the Google Earth Pro platform available from the chosen years, 150 were from the mangrove class and 150 from the others class derived from the union of the other classes. With the objective of better visualizing the alterations suffered by the mangrove class over the years, 10-year analyses were carried out, divided into 5-year intervals, corresponding to the years of 2010, 2015 and 2020.

For the mapping carried out for the year of 2010, out of a total of 300 points, 290 were correctly classified, reaching an accuracy of 96.67% and a Kappa index of approximately 93%. Of the 150 mangrove class reference points, 143 were correctly classified, indicating a producer accuracy of 95.33% and a user accuracy of 97.95%. According to the methodology of Pontius and Millones (2011), the errors generated disagreements of 3.33%, for the positional classification and quantity classification (Table IVa).

The error matrix for the year of 2015 shows that 291 points were classified correctly, out of a total of 300 points, reaching an accuracy of 97% and a Kappa index of approximately 94%. Of the 150 mangrove class reference points, 143 were classified correctly, indicating a producer accuracy of 95.33% and user accuracy of 98.62%, with a total disagreement of 3.0% (Table IVb).

As in the year 2010, for the images of the year 2020, out of a total of 300 points, 290 were classified correctly, reaching an accuracy of 96.67% and a Kappa index of 93.33%. Considering the 150 reference points of the mangrove class, 143 were correctly classified, which shows a producer accuracy of 95.33% and user accuracy of 97.95%. The observed errors indicate disagreements of 3.33% (Table IVc).

4.3. Change detection in mangrove areas

The change detection was obtained through the intersect tool as described in the methodology, where it was possible to obtain the areas that remained unchanged, reduced and expanded, from the largest time interval that the present work addresses – from the year 2010–2020. As the main objective was to analyze the mangrove areas, the other classes were grouped, analyzing only the mangrove class.

The changes that occurred in the study area are shown in Fig. 6a, through a change detection map, showing the areas that were lost, expanded and those that were maintained and not changed over the 10 years.

Statistically, assuming that the total area has 119.5 km^2 when analyzing the mapped data from 2010 to 2020, we realize that an area of 2170 km^2 (12%) was occupied by mangrove forests; however, 1706 km^2 (9%) of mangroves were reduced, while an area of 14,422 km^2 (79%) did not change and remained preserved and/or unchanged. Fig. 6b and c shows the altered and unaltered areas of mangroves and their corresponding percentage.

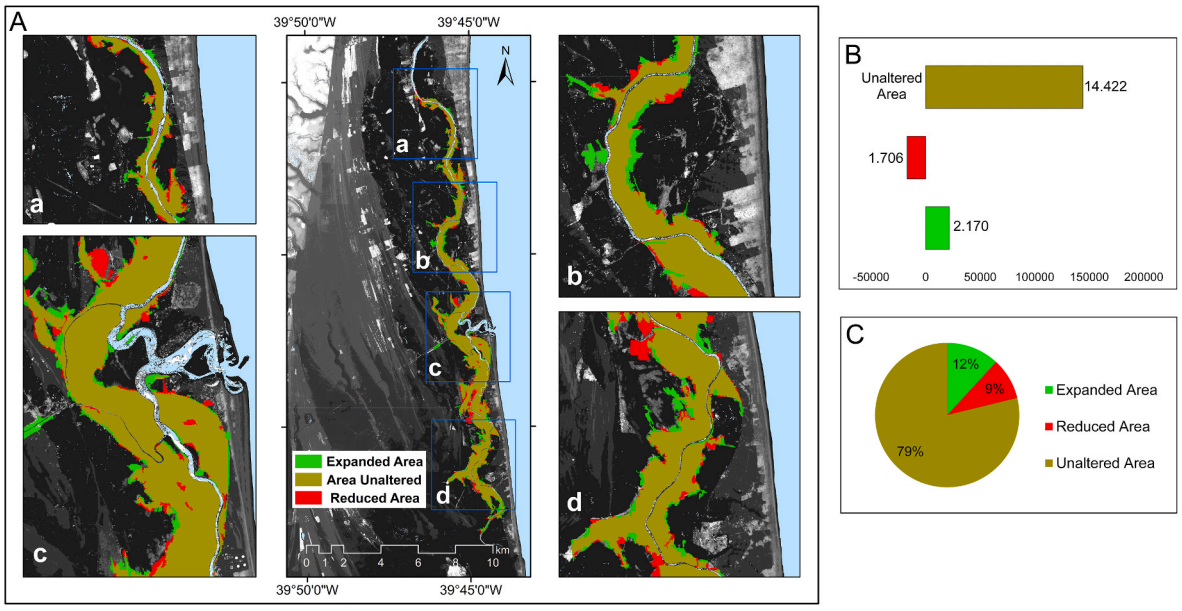

Fig. 6. a- Unaltered mangrove areas, mangrove areas that underwent expansion and reduction. b- Unaltered, reduced and expanded mangrove areas, in m^2, c- Balance in percentage of mangroves in the 10-year time interval, showing that over time the area lost 9.0% of the mangrove areas.

5. Discussions

The mapping carried out includes the main areas of occurrence of mangroves in the district of Barra Nova, city of São Mateus, using recent tools that are well accepted in the scientific community. The results are excellent, according to the global accuracy number (Story and Congalton, 1986) and the Kappa index (Congalton and Green, 2019), in addition to the low values of quantity and allocation disagreements (Pontius and Millones, 2011), considering the intervals of five years (2010, 2015 and 2020) for the last decade.

Spatial data on the distribution, oceanographic studies, composition, and condition of mangroves, considering at appropriate spatial scales, is essential to support the understanding, as well as the management of mangrove ecosystems and their biodiversity, for instance, using remote sensing analysis (Kamal et al., 2015; Kundal et al., 2023), and also new technologies such as drones (Cohen et al., 2023).

The results are justified by the good images of the CBERS sensors used in the classification, achieving a resolution of 20, 5 and even 2 m, when applied to the pre-processing techniques in the images. Furthermore, the 2 m mesh digital elevation allowed us to differentiate the small elevations in the coastal plain that occur in the area, distinguishing the regions of low vegetation from those areas with the presence of exuberant vegetation, represented by the well-developed mangroves.

When comparing the mapping data from the present study for the years 2010–2015 (16.77 km^2), considering an average, we identified similarities with the mapping published by (IEMA, 2015) and carried out between the intervals of the years 2012–2015 (16.48 km^2). Thus, the works can be analyzed and compared, as they were prepared at the same scale. The classification presented in the present work, however, allowed greater refinement with the use of the GEOBIA methodology, which compartmentalizes and classifies into objects (areas), just as the human mind analyzes all information and positions in space to better define the object and classify it.

The expansion of mangrove forests between the years 2010 and 2015 identified in the work is also found in the IEMA studies, which associated the growth of mangroves along the Mariricu river drainage network with coastal dynamics and climate change, which causes losses and gains of mangroves through natural variations. During this period, a strong drought was observed, more severely affecting the river basins in the north of the State of Espírito Santo, where in the dry period the region's rivers lost their water discharge power and their beds were invaded by sea water, causing soil salinization and expanding the favorable environments for the expansion of mangroves.

The works by Nascimento Jr, (2016) and Lopes (2020) revealed that mangroves in coastal regions in Brazil remain in a good state of preservation, establishing more gains than losses. For the clipping of the study region, this similarity continues, because despite the variation in the mangrove fields, the areas of gain are greater than the areas of loss, in addition to the confirmation of unaltered areas.

5.1. Mangrove changes and coastal services

Several studies have provided mapping and change detection in mangrove areas (Saenger et al., 1983; Giri et al., 2011; Diniz et al., 2019). Therefore, in order to contribute to global mangrove studies, our data also present a mangrove change, reinforcing the great importance of understanding the coastal dynamic and its impacts on biodiversity and human communities.

Basically, the changes in mangrove distribution may have resulted from sedimentary variables (Moraes et al., 2017; Ribeiro et al., 2018), as well as sea level fluctuations (Cohen et al., 2012; França et al., 2012, 2016; Bozi et al., 2021; Nunes et al., 2023), climate and hydrology changes (Azevedo et al., 2021; Rodrigues et al., 2022), and anthropogenic actions.

The development of mangroves is regulated by continent-ocean interactions and their expansion is determined by the topography relative to sea-level (Gornitz, 1991; Lara and Cohen, 2006), and flow energy (Chapman, 1976; Woodroffe et al., 1989), where mangroves preferentially occupy mud surfaces. Thus, a relative rise in sea-level may result in mangroves migrating inland due to changes in flow energy and tidal inundation frequency. Similarly, vegetation on elevated mudflats is subject to boundary adjustments, since mangroves can migrate to higher locations and invade these areas (Lara and Cohen, 2006). Obviously, the potential of each variable to influence mangrove establishment will depend on the environmental characteristics of the given littoral.

Climate fluctuations promote impacts in rainfall (Molodkov and Bolikhovskaya, 2002), and consequently could also cause changes in river flow, and estuarine salinity gradients (Lara and Cohen, 2006). Therefore, this can also affect the RSL, as well as cause direct effects in mangrove distributions (Cohen et al., 2014).

In general, mangroves have many pivotal roles, such as bio-indicators, as well as coastal change indicators, and also because they control exchanges of materials at the interfaces between land, atmosphere, and ocean ecosystems. They provide coastal protection by mitigating erosion and storm surge, and also promote food security to coastal inhabitants, providing nursery grounds for commercial fish and food resources (Alongi, 2002; Barbier et al., 2011).

Therefore, mangroves are one of the key ecosystems that can contribute to climate change mitigation (Mcleod et al., 2011; Duarte and Arabia, 2017; Howard et al., 2017), as well as mangrove systems play an essential role in human sustainability, providing a wide range of ecosystem services.

6. Conclusion

The work developed shows that we can combine data from Brazilian remote sensors, such as CBERS, with the use of GEOBIA techniques in the study of a specific area of interest and not just in areas of large territorial dimensions; and by this method we can reach satisfactory and reliable results. Thus, in a decade, a coastal region underwent changes in its mangrove area, showing a tendency to growth, but punctuating variations in the 5-year time intervals.

Currently, society increasingly needs to obtain information about its environments, seeking to understand their changes as well as the consequences of these changes for biodiversity. Therefore, studies of this nature are of great scientific, social, educational and economic relevance, as they aim to contribute to decision-making for better management of coastal environments.

CRediT authorship contribution statement

Débora Cristina de Lima Miranda: Conceptualization, Formal analysis, Investigation, Writing – original draft, Writing – review & editing. **Marlon Carlos França:** Conceptualization, Formal analysis, Funding acquisition, Investigation, Project administration, Supervision, Writing – original draft, Writing – review & editing. **Luke Ortiz-Whittingham:** Writing – original draft, Writing – review & editing. **Laurent Polidori:** Formal analysis, Writing – original draft, Writing – review & editing.

Declaration of competing interest

The authors declare that they have no known competing financial interests or personal relationships that could have appeared to influence the work reported in this paper

Data availability

Data will be made available on request.

Acknowledgments

We would like to thank the members of the Laboratory of Coastal Dynamics (LADIC-UFPA), Graduate Program in Geology and Geochemistry – PPGG, Federal University of Pará, and Laboratory of Oceanography and Climate, Federal Institute of Espírito Santo - Campus Piúma for their support. This study was financed by the Fundação de Amparo à Pesquisa e Inovação do Espírito Santo – FAPES (093/2020, 03/2021, 282/2021, 441/2021, 417/2022, 850/2022, and 1034/2022), and in part by the Coordenação de Aperfeiçoamento de Pessoal de Nível Superior – Brasil (CAPES) - Finance Code 001. The second author would like to thank CNPq for research scholarship (309618/2020-7).

References

Alongi, D.M., 2002. Present state and future of the world's mangrove forests. Environ. Conserv. 29, 331–349.

Alongi, D.M., 2008. Mangrove forests: resilience, protection from tsunamis, and responses to global climate change. Estuar. Coast Shelf Sci. 76 (1), 1–13. https://doi.org/10.1016/j.ecss.2007.08.024.

Alongi, D.M., 2012. Carbon sequestration in mangrove forests. Carbon Manag. 3 (3), 313–322. https://doi.org/10.4155/cmt.12.20.

Alongi, D.M., 2015. The impact of climate change on mangrove forests. Curr. Clim. Change Rep. 1 (1), 30–39.

Antunes, D.A., 2015. Análise orientada a objeto geográfico na caracterização do uso e ocupação da terra em segmentos do rio Pitangui, Paraná: avaliações preliminares. MS Dissertation, Instituto de Geociências, Universidade do Estado de Ponta Grossa, p. 140p.

Azevedo, A., Jiménez-Espejo, F., França, M., García-Alix, A., Silva, F., Pessenda, L., Cohen, M., Fontes, N., Pinheiro, V., Macario, K., Melo Jr., J., Piccolo, M., Bendassolli, J., 2021. Hydrological influence on the evolution of a subtropical mangrove ecosystem during the late Holocene from Babitonga Bay, Brazil. Palaeogeogr. Palaeoclimatol. Palaeoecol. 574, 110463.

Barbier, E.B., Hacker, S.D., Kennedy, C., Koch, E., Stier, A., Silliman, andB.R., 2011. The value of estuarine and coastal eco-system services. Ecol. Monogr. 81, 169–193.

Bezerra, D., Santos, A., Amaral, Kampel, M., Anderson, L., Mochel, F., Nunes, J., Araujo, N., Barreto, L., Pinheiro, M., Celeri, M., Silva, F., Viegas, A., Manes, S., Rodrigues, T., Viegas, J., Souza, U., Santos, A., Silva-Junior, C., 2022. Brazil's mangroves: natural carbon storage. Science 375, 6586. https://doi.org/10.1126/science.abo4578.

Blasco, F., Saenger, P., Janodet, E., 1996. Mangroves as indicators of coastal change. Catena 27, 167–178.

Bozi, B., Figueiredo, B., Rodrigues, E., Cohen, M., Pessenda, L., Alves, E., Souza, A., Bandassolli, J., Macario, K., Azevedo, P., Culligan, N., 2021. Geomorphology 390, 107860.

Buso Junior, A.A., Pessenda, L.C.R., Oliveira, P.E.O., Giannini, P.C.F., Cohen, M.C.L., Ribeiro, C.V., Oliveira, S.M.B., Favaro, D.I.T., Rossetti, D.F., Lorente, F.L., Borotti Filho, M.A., Schiavo, J.A., Bendassolli, J.A., França, M.C., Guimaraes, J.T.F., Siqueira, G.S., 2013. Late pleistocene and holocene vegetation, climate Dynamics, and amazonian taxa in the atlantic rainforest of linhares, southeastern Brazil. Radiocarbon 55, 1747–1762.

Carvalho, L.M.V., Jones, C., Liebmann, B., 2004. The South Atlantic convergence zone: intensity, form, persistence, and relationships with intraseasonal to interannual activity and extreme rainfall. J. Clim. 17, 88–108.

Carvalho, M. V. A. de, Silva, G. F. da, Cruz, C.B.M., Almeida, P. M. M. de, 2015. Avaliação do mapeamento de manguezais na região Metropolitana do Rio de Janeiro através da integração entre GEOBIA e mineração de dados. In: INPE, 17°, Simpósio Brasileiro de Sensoriamento Remoto - SBSR, Anais[...]. João Pessoa, v1, pp. 6381–6388.

Castro, D.F., Rossetti, D.F., Cohen, M.C.L., Pessenda, L.C.R., Lorente, F.L., 2013. The growth of the Doce River Delta in northeastern Brazil indicated by sedimentary facies and diatoms. Diatom Res. 28 (4), 455–466. https://doi.org/10.1080/0269249X.2013.841100.

Chapman, V.J., 1976. Mangrove Vegetation. Velag Von J. Cramer, Leutershausen, Germany, p. 447.

Chavez, P.S., 1988. An improved dark-object subtraction technique for atmospheric scattering correction of multispectral data. Remote Sensing of Environment 24 (3), 459–479. https://doi.org/10.1016/0034-4257(88)90019-3.

Cohen, M., Souza, A., Kam-Biu, L., Qiang, Y., 2023. A timely method for post-disaster assessment and coastal landscape survey using drone and satellite imagery. MethodsX 10, 102065.

Cohen, M.C.L., França, M.C., Rossetti, D.de F., Pessenda, L.C.R., Giannini, P.C.F., Lorente, F.L., Buso Junior, A.Á., Castro, D., Macario, K., 2014. Landscape evolution during the late quaternary at the Doce River mouth, Espírito Santo state, southeastern Brazil. Palaeogeogr. Palaeoclimatol. Palaeoecol. 415, 48–58. https://doi.org/10.1016/j.palaeo.2013.12.001.

Cohen, M.C.L., Pessenda, L.C.R., Behling, H., Rossetti, D.de F., França, M.C., Guimarães, J.T.F., Friaes, Y., Smith, C.B., 2012. Holocene palaeoenvironmental history of the Amazonian mangrove belt. Quat. Sci. Rev. 55, 50–58. https://doi.org/10.1016/j.quascirev.2012.08.019.

Congalton, R.G., 1991. A review of assessing the accuracy of classifications of remotely sensed data. Remote Sensing of Environment 37 (1), 35–46.

Congalton, R.G., Green, K., 2019. Assessing the Accuracy of Remotely Sensed Data Principles and Practices, 3 ed. Taylor & Francis Group, Boa Raton.

Desclée, B., Bogaert, P., Defourny, P., 2006. Forest change detection by statistical object-based method. Remote Sensing of Environment 102 (1–2), 1–11.

Diniz, C., Cortinhas, L., Nerino, G., Rodrigues, J., Sadeck, L., Adami, M., Souza-Filho, P. W.M., 2019. Brazilian mangrove status: three decades of satellite data analysis. Rem. Sens. 11 (7) https://doi.org/10.3390/rs11070808.

Duarte, C.M., Arabia, S., 2017. Reviews and syntheses: hidden forests, the role of vegetated coastal habitats in the ocean carbon budget. Biogeosciences 301–310.

Duke, N.C., Ball, M.C., Ellison, J.C., 1998. Factors influencing biodiversity and distributional gradients in mangroves. Global Ecol. Biogeogr. Lett. 7 (1), 27–47.

Eugenio, F.C., Santos, A. R.dos, Fiedler, N.C., Ribeiro, G.A., Silva, A. G.da, Soares, V.P., Gleriani, J.M., 2017. Mapeamento das áreas de preservação permanente do estado do Espírito Santo, Brasil. Ciência Florest. 27 (3), 897–906. https://doi.org/10.5902/1980509828639.

Felgueiras, C.A., 2001. Modelagem ambiental com tratamento de incertezas em sistemas de informação geográfica: o Paradigma Geostatístico por indicação. Instituto Nacional De Pesquisas Espaciais (INPE).
França, M.C., Francisquini, M.I., Marcelo, C.L.C., Pessenda, L.C.R., Rosseti, D.F., Guimaraes, J.T.F., Smith, C.B., 2012. The last mangroves in marajó island – eastern amazon: climate and/or relative seasea-level changes impacts. Rev. Palaeobot. Palynol. 187, 50–68. https://doi.org/10.1016/j.revpalbo.2012.08.007.
França, M.C., Alves, I.C.C., Cohen, M.C.L., Rossetti, D.F., Pessenda, L.C.R., Giannini, P.C. F., Lorente, F.L., Buso Junior, A.Á., Bendassolli, J.A., Macario, K., 2016. Millennial to secular time-scale impacts of climate and sea-level changes on mangroves from the Doce River delta, Southeastern Brazil. Holocene 26 (11), 1733–1749. https://doi.org/10.1177/0959683616645938.
Freitas, D. M. de, Ramos, A.L. de A., Sano, E.E., Resende, K.B., Fumi, M., Oliveira, F. F. G. de, V. B, Q., 2017. Mapeamento de manguezais e carcinicultura do Brasil com base em imagens dos satélites Landsat-8 OLI e RapidEye (ano-base: 2013). In: INPE, 18°, Símposio Brasileiro de Sensoriamento Remoto - SBSR, Anais[...]. Santos,SP v.1, pp. 81–109.
Friess, D.A., Rogers, K., Lovelock, C.E., Krauss, K.W., Hamilton, S.E., Lee, S.Y., Lucas, R., Primavera, J., Rajkaran, A., Shi, S., 2019. The state of the world's mangrove forests: past, present and future. Annu. Rev. Environ. Resour. 44, 89–115. https://doi.org/10.1146/annurev-environ-101718-033302.
Fromard, F., Vega, C., Proisy, C., 2004. Half a century of dynamic coastal change affecting mangrove shorelines of French Guiana. A case study based on remote sensing data analyses and field surveys. Mar. Geol. 208 (2–4), 265–280. https://doi.org/10.1016/j.margeo.2004.04.018.
Giri, C., Ochieng, E., Tieszen, L.L., Zhu, Z., Singh, A., Loveland, T., Masek, J., Duke, N., 2011. Status and distribution of mangrove forests of the world using earth observation satellite data. Global Ecol. Biogeogr. 20 (1), 154–159. https://doi.org/10.1111/j.1466-8238.2010.00584.x.
Gornitz, V., 1991. Global coastal hazards from future sea level Rise. Palaeogeogr. Palaeoclimatol. Palaeoecol. 89, 379–398.
Hamylton, S., Kelleway, J., Rogers, K., McLean, R., Tynan, Z.N., Repina, O., 2023. Mangrove expansion on the low wooded islands of the Great Barrier Reef. Proc. R. Soc. A B 290, 20231183. https://doi.org/10.1098/rspb.2023.1183.
Hatje, V., Masqué, P., Patire, V., Dórea, A., Barros, F., 2021. Blue carbon stocks, accumulation rates, and associated spatial variability in Brazilian mangroves. Limnol. Oceanogr. 66 (2), 321–334.
Hay, G.J., Castilla, G., 2008. Geographic object-based image analysis (GEOBIA): a new name for a new discipline. Lecture Notes in Geoinformation and Cartography 0 (9783540770572), 75–89. https://doi.org/10.1007/978-3-540-77058-9_4.
Hidayatullah, M.F., Kamal, M., Wicaksono, P., 2023. Species-based aboveground mangrove carbon stock estimation using WorldView-2 image data. Remote Sens. Appl.: Society and Environment 30, 100959.
Howard, J., Sutton-Grier, A., Herr, D., Kleypas, J., Landis, E., Mcleod, E., Pidgeon, E., Simpson, S., 2017. Clarifying the role of coastal and marine systems in climate mitigation. Front. Ecol. Environ. 15 (1), 42–50. https://doi.org/10.1002/fee.1451.
ICMBio, 2018. Atlas Dos Manguezais Do Brasil, first ed. ICMBio: Brasilia, Brazil. 2018; ISBN 978-85-61842-75-8.
IEMA, 2015. Referência Técnica Contrato : 001/2012 Processo No 54137624/2011 Edital Concorrência No 002/2011 Contratante : Instituto Estadual de Meio Ambiente e Recursos Hídricos – IEMA Objeto : Contratação de empresa especializada em Engenharia Cartográfica pa.
Kamal, M., Phinn, S., Johansen, K., 2015. Object-based approach for multi-scale mangrove composition mapping using multi-resolution image datasets. Rem. Sens. 7 (4), 4753–4783.
Kathiresan, K., Rajendran, N., 2005. Mangrove ecosystems of the Indian Ocean region. Indian J. Mar. Sci. 34 (1), 104–113.
Kristensen, E., Bouillon, S., Dittmar, T., Marchand, C., 2008. Organic carbon dynamics in mangrove ecosystems: a review. Aquat. Bot. 89 (2), 201–219. https://doi.org/10.1016/j.aquabot.2007.12.005.
Kundal, S., Chowdhury, A., Bhardwaj, A., Garg, P.K., Mishra, V., 2023. GeoBIA-based semi-automated landslide detection using UAS data: a case study of Uttarakhand Himalayas. SPIE Future Sensing Technologies 2023 12327, 321–329 (SPIE).
Lara, J.R., Cohen, M.C.L., 2006. Sediment porewater salinity, inundation frequency and mangrove vegetation height in Bragança, North Brazil: an ecohydrology-based empirical model. Wetl. Ecol. Manag. 4, 349–358.
Latorre, M., Carvalho Júnior, O. A. de, Carvalho, A.P.F., Shimabukuro, Y.E., 2002. Correção atmosférica: conceitos e fundamentos. Espaço & Geografia 5 (1), 153–178.
Leonardi, F., Oliveira, C., 2009. Fusão de imagens CBERS 2B: ccd-hrc. In: INPE, 14° Simpósio Brasileiro de Sensoriamento Remoto (SBSR), Anais[...], pp. 6951–6958. Natal. http://marte.dpi.inpe.br/col/dpi.inpe.br/sbsr@80/2008/11.16.12.28/doc/6951-6958.pdf.
Lopes, J.P.N., 2020. Duas décadas de mudanças dos manguezais de meso e micromarés do litoral brasileiro a partir de imagens multisensores. MS Dissertation. Programa de Pos Graduação em Geologia e Geoquímica, Instituto de Geociências, UFPA, Belém-Pa, xii, p. 32.
Mcleod, E., Chmura, G.L., Bouillon, S., 2011. Ablueprint for blue carbon: toward an improved under-standing of the role of vegetated coastal habitats in seques-tering CO2. Front. Ecol. Environ. 9, 552–560.
Meneses, P.R., Almeida, T. de, 2012. Introdução ao processamento de imagem de sensoriamento remoto. Brasília,DF, Cnpq/Unb. org.
Molodkov, A.N., Bolikhovskaya, N.S., 2002. Eustatic sea-level and climate changes over the last 600 ka as derived from molluskbased ERS-chronostratigraphy and pollen evidence in Northern Eurasia. Sediment. Geol. 150, 185–201.
Moraes, C., Fontes, N., Cohen, M., França, M., Pessenda, L., Rossetti, D., Francisquini, M., Bendassolli, J., Macario, K., 2017. Late Holocene mangrove dynamics dominated by autogenic processes. Earth Surf. Process. Landforms 42 (13), 2013–2023.
Moses, W.J., Sterckx, S., Montes, M.J., Keukelaere, L.de, Knaeps, E., 2017. Atmospheric correction for inland waters. In: Bio-optical Modeling and Remote Sensing of Inland Waters. Proceedings[. Elsevier, pp. 69–100. https://doi.org/10.1016/B978-0-12-804644-9.00003-3.
Nascimento Jr, W.R., 2016. Análise da dinâmica das áreas de manguezal no litoral Norte do Brasil a partir de dados multisensores e hidrossedimentológicos. Phd Thesis. Programa de Pós-Graduação em Geologia e Geoquímica, Universidade Federal do 132–p.
Nascimento, W., Souza-Filho, P.W.M., Proisy, C., Lucas, R.M., Rosenqvist, A., 2013. Mapping changes in the largest continuous Amazonian mangrove belt using object-based classification of multisensor satellite imagery. Estuar. Coast Shelf Sci. 117, 83–93. https://doi.org/10.1016/j.ecss.2012.10.005.
Nunes, S., França, N., Cohen, M., Pessenda, L., Rodrigues, E., Magalhães, E., Silva, F., 2023. Assessment the impacts of sea-level changes on mangroves of ceará-mirim estuary, northeastern Brazil, during the holocene and anthropocene. Plants 12, 1721. https://doi.org/10.3390/plants12081721.
Pontius, R.G., Millones, M., 2011. Death to Kappa: birth of quantity disagreement and allocation disagreement for accuracy assessment. Int. J. Rem. Sens. 32 (15), 4407–4429. https://doi.org/10.1080/01431161.2011.552923.
Ribeiro, S., Batista, E., Cohen, M., França, M., Pessenda, L., Fontes, N., Alves, I., Bendassolli, J., 2018. Allogenic and autogenic effects on mangrove dynamics from the Ceará Mirim River, north-eastern Brazil, during the middle and late Holocene. Earth Surf. Process. Landforms 43 (8), 1622–1635.
Rodrigues, E., Cohen, M., Pessenda, L., França, M., Magalhães, E., Yao, Q., 2022. Poleward mangrove expansion in South America coincides with MCA and CWP: a diatom, pollen, and organic geochemistry study. Quat. Sci. Rev. 288, 107598 https://doi.org/10.1016/j.quascirev.2022.107598.
Rossetti, D. de F., Polizel, S.P., Cohen, M.C.L., Pessenda, L.C.R., 2015. Late Pleistocene–Holocene evolution of the Doce River delta, southeastern Brazil: implications for the understanding of wave-influenced deltas. Mar. Geol. 367, 171–190. https://doi.org/10.1016/j.margeo.2015.05.012.
Saenger, P., Hegerl, E.J., Davie, J.D.S., 1983. Global Status of Mangrove Ecosystems. International Union for Conservation of Nature and Natural Resources: Gland, Switzerland.
Schaeffer-Novelli, Y., Cintrón-Molero, G., Adaime, R.R., Camargo, T. M.de, 1990. Variability of mangrove ecosystems along the Brazilian coast. Estuaries 13 (2), 204–218. https://doi.org/10.2307/1351590.
Silva, F., França, M., Cohen, M., Pessenda, L., Mayle, F., Fontes, N., Lorente, F., Buso-Junior, A., Piccollo, M., Bendassolli, J., Macario, K., Culligan, N., 2022. Late Holocene mangrove dynamics of the Doce River delta, southeastern Brazil: implications for the understanding of mangrove resilience to sea-level changes and channel dynamics. Palaeogeogr. Palaeoclimatol. Palaeoecol. 600, 111055 https://doi.org/10.1016/j.palaeo.2022.111055.
Silva, F., Pantoja, N., Torres, A., Ortiz-Whittingham, L., Vanconcellos, A., Nascimento, N., Machado, G., Rocha, P., Orijemie, E.A., França, M., 2023. Palynology: a forensic trace tool to identify a temporal coastal vegetation changes. Revista Ifes Ciência 9 (3), 1–11. https://doi.org/10.36524/ric.v9i3.2258.
Story, M., Congalton, R.G., 1986. Accuracy assessment: a user's perspective. Photogramm. Eng. Rem. Sens. 52 (3), 397–399.
Suguio, K., Martin, L., Bittencourt, A.C.S., Dominguez, J.M.L., Flexor, J.M., Azevedo, A. E. G. de, 1985. Flutuações do nível relativo do mar durante o quaternário superior ao longo do litoral brasileiro e suas aplicações na sedimentação costeira. Rev. Bras. Geociencias 15 (4), 273–286. http://www.ppegeo.igc.usp.br/index.php/rbg/article/view/12026/11570.
Tomlinson, P.B., 1986. The Botany of Mangroves. Cambridge University Press, Cambridge.
Van der Stocken, T., Carroll, D., Menemenlis, D., Simard, M., Koedam, N., 2019. Global-scale dispersal and connectivity in mangroves. Proc. Natl. Acad. Sci. U.S.A. 116 (3), 915–922. www.pnas.org/cgi/doi/10.1073/pnas.1812470116.
Weckmüller, R., Vicens, R.S., 2013. Análise temporal da cobertura da terra do município de Petrópolis/RJ numa abordagem pós-classificação de detecção de mudanças. Revista Brasileira de Geografia Física 6, 1275–1291.
Woodroffe, C.D., Chappell, J., Thom, B.G., Wallensky, E., 1989. Depositional model of a macrotidal estuary and floodplains, South Alligator River, Northern Australia. Sedimentology 36, 737–756.
Woodroffe, C., Nicholls, R.J., Birkett, V., et al., 2014. The impact of climate change on coastal ecosystems. In: Oceans and Human Health: Implications for Society and Well-Being. Wiley Blackwell.
Trimble. 2014. eCognition advanced geospatial data analysis. Disponível em: https://geospatial.trimble.com/what-is-ecognition. Acesso em: 26/06/2020.